4th. International Congress on Civil Engineering , Architecture and Urban Development
27-29 December 2016, Shahid Beheshti University , Tehran , Iran

MITIGATION OF GROUND VIBRATIONS INDUCED BY HIGH-SPEED TRAIN

Mojtaba Ghobakhlou*[1] , Leena Korkiala-Tanttu[2]

1. PhD candidate, Aalto University, Finland, mojtaba.ghobakhlou@aalto.fi,
*.Corresponding author, Telephone: +358 465253413
2. Professor of Geoengineering, Aalto University, Finland, leena.korkiala-tanttu@aalto.fi

Abstract

This paper presents a model about using a concrete wave barrier for mitigation of ground vibrations induced by a high- speed train. The paper considers a numerical model which was divided into two parts. In the first part, time dependent reaction of a recorded point during train movement was modeled. The model included concentrated moving loads at constant velocity on an elastic beam with spring supports. In the second part, the results of the first part were applied as input data of loading. The aim of this paper was to evaluate the dynamic behavior of a subsoil layer during wave propagation before and after constructing a wave barrier. The wave barrier mitigated 12 to 17 percent of the vibrations in the distance of 30m to 40m in the upper part of the subsoil respectively. This indicated that the wave barrier reflected and also absorbed some component of waves. The mitigated maximum total velocities fulfilled the accepted level of vibration.

Key words: Concrete wave barrier, Ground vibrations, High-speed trains, Numerical model, Time dependent reaction, Wave propagation.

1. Introduction

The use of fast transportation systems is growing because of the development of technology and the increase of Earth population. A high-speed train has a beneficial capacity to transit lots of passengers in a short period of time in comparison with other transportation systems. However, a high-speed train propagates noises and vibrations. The vibrations annoy people living in the vicinity of railroads. Moreover, excessive vibrations can cause damage both to the foundations and buildings. Thus, many researchers have investigated the high-speed train movement and the ground vibrations. They have carried out numerous laboratory experiments, in-situ tests, and numerical models to reduce the ground vibrations. A few of their findings are reviewed here.

Hall [1] developed an investigation model depending on the actual vibrations. To measure actual vibrations, he used extensometers. Extensometers recorded the vertical deflection of embankments, particle acceleration in the embankments, and particle velocity in the surrounding. The extensometers data were compared with numerical results. However, he only considered the data of a train with 142 km/h speed. In another study, Koivisto et al. [2] studied the impact of deep stabilization columns to reduce ground vibration. They implemented an impact method and a sinusoidal method for modelling the dynamic load. Although the deep stabilization columns decreased the ground vibration, their modelling considered only low-speed train.

Buonstani et al. [3] presented a model to reduce the ground vibrations through the use of barriers. The model included only the axles of a locomotive as a moving load. The suggested load distribution was not realistic because the impact of the carriages load was neglected. Recent research by With et al. [4] demonstrated that a wave barrier of lime-cement columns which were constructed parallel to the track can reduce the maximum particle velocity.

Costa et al. [3] divided the numerical model into two main modules. The first module contained the track-ground structure, modelled by a two-dimensional approach considering a three-dimensional nature of the domain. The second module consisted of the dynamic behavior of a train. It was simulated by a multi-body formulation considering the main masses and suspensions of the vehicles. Based on the coupling between the finite elements (FEM) and boundary elements (BEM) methods, the track-ground dynamic response induced by the train passage was computed. Paolucci et al. [4] applied a spectral element method to simulate the ground motion induced by the passage of an X-2000 passenger train at the test site of Ledsgaard, Sweden.

A lot of primary researches have been conducted to obtain the critical velocity of train which induce high ground vibrations. Krylov [5] concluded in his theoretical studies that maximum ground vibration occurred when the velocity of a high speed train approximately achieved the velocity of Rayleigh waves in the ground. In a study done by Madshus and Kaynia [6], results from instrumented tests with a high speed train on a soft soil site in Sweden indicated that the critical speed was controlled by the minimum phase velocity of the first soil Rayleigh mode. Moreover, the critical speed and the amount of dynamic amplification depended also on a coincidence between characteristic wave lengths for the site and the distances between bogies and axles in the train.

Forrest and Hunt [7] used a 3D tunnel model to assess the effectiveness of a floating-slab track, and to evaluate the soil vibration due to random roughness-displacement excitation between the masses and the rail beam. Karlstrom and Bostrom [8] adopted a full 3D analytical approach to account trenches close to a railroad by considering train-induced low-frequency ground vibrations. The ground was modelled as a layered semi-infinite domain and the embankment with finite layers, and no irregularities in rails or wheels were accounted for. Galvin and Dominguez [9] used a 3D boundary element method and finite element approach for the analysis of train induced vibrations. They compared experimental and numerical results at several points near the track. The scaled boundary finite-element method (SBFEM) was applied by Yaseri et al. [10] to implement the 3D analysis of ground vibrations induced by underground trains. The media around the tunnel was simulated by the SBFEM.

The purpose of this paper is to evaluate the dynamic behavior of subsoil during wave propagation before and after constructing a concrete wave barrier. To achieve the target, this paper introduces a 2D axisymmetric method analysis of ground vibration induced by high-speed train with the following hypothesis: both the steel railroad and the concrete sleepers were assumed to be constant along the track. The track was considered to behave in a linear fashion, and also the concrete was taken to have a linear-elastic behavior and to be un-cracked. Therefore, lateral forces, lateral accelerations or displacements were not considered. The dynamic responses focused on vertical accelerations, vertical displacements, vertical velocities and also particle velocities. The train was supposed to cross the track at constant speed, and was modelled with moving axle loads. Given the assumptions above, several factors were omitted from this research, such as track irregularities, snow load, water pressure, and wind load. Only the subsoil which behaved elastic on dynamic analysis was considered. On boundary conditions, the level of the ground water was assumed to be lower than the level of bottom boundary. The parts of wave propagation from source to destination are described in section 2. The simulation and its details are defined in section 3. The results of numerical modelling are discussed in section4. Finally, the impact of using wave barrier is concluded in section 5.

2. Modelled objects

As shown in Fig. 1, the problem can be subdivided into four parts: source, path, barrier, and observation points.

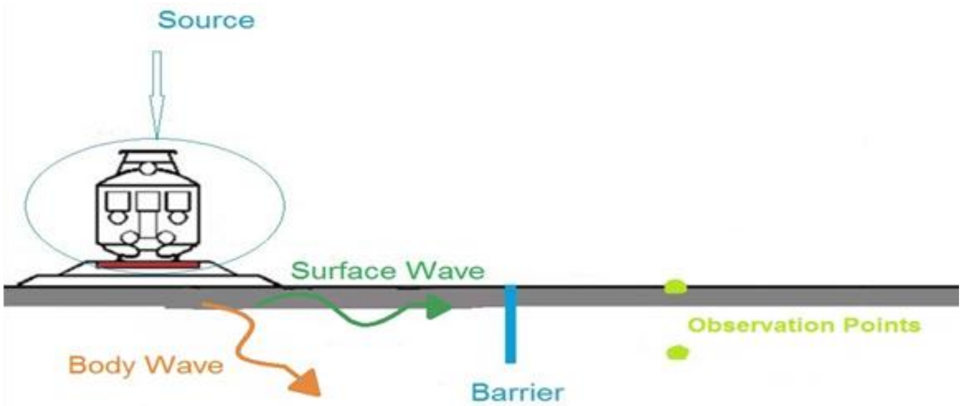

Figure1 , the case study components. Source: train+ railway, Path: embankments+ subsoil, Barrier: concrete wave barrier, and observation points.

Source

In this case study, the source includes: train, rails and sleepers. As indicated in Fig. 1, the source propagates body waves and surface waves. The body waves can travel through the inside of the path. While, the surface waves can travel only through the upper part of soil.

Path

This part includes: a ballast layer, a sub-ballast layer and a subsoil layer. Generally, being generated in the source, the waves propagate in the path and pass the ballast and the sub-ballast layer. In this paper, the effectiveness of vibrations in the ballast and sub-ballast is not considered, only the impact of the vibrations in the subsoil is taken into account.

Barrier

A concrete wave barrier is used to isolate and reduce the ground vibrations. Due to high differences of impedances in comparison to the soil layer, this concrete barrier is capable of reflecting the part of propagated wave back to the subsoil.

Observation Points

To evaluate and study the behavior of the soil layer in two different types of vibrations with and without barrier, the observation points are used. These points with the relevant details of their distances from the source and positions are discussed in section 4.

3. Model simulation

A 2-dimensional model was applied instead of using a 3-dimensional model. In the first subsection, to find a function of velocity during the period of train movement, an elastic beam with spring supports was simulated. In the second subsection, the results of the first subsection was used to define the vibration in each part of the subsoil.

Simulation of a train movement

The geometry and axle loads of the high-speed train X2000 was used to simulate the high-speed train movement. The train was designated for the speed up to 270 km/h (130 mph). In this case the train movement on railroad with 200 km/h speed was modelled with Abaqus. The reaction point (RP) which was located 30 meter from the head train collected the responses of train movement. The point is shown as "RP" recorded the dynamic variation of displacement, velocity and acceleration during the train movement, Fig. 2.
The goal of source modelling was to obtain the time function of velocity in RP. By using the velocity results, it was possible to model wave propagation problems in a 2-dimensional space instead of a 3d problem which was time consuming and needed lots of parameters. The train movement on railway was modelled as concentrated moving load with constant velocity on an elastic beam which was supported with spring constraints. Each spring had a distance of 500 mm from the other.

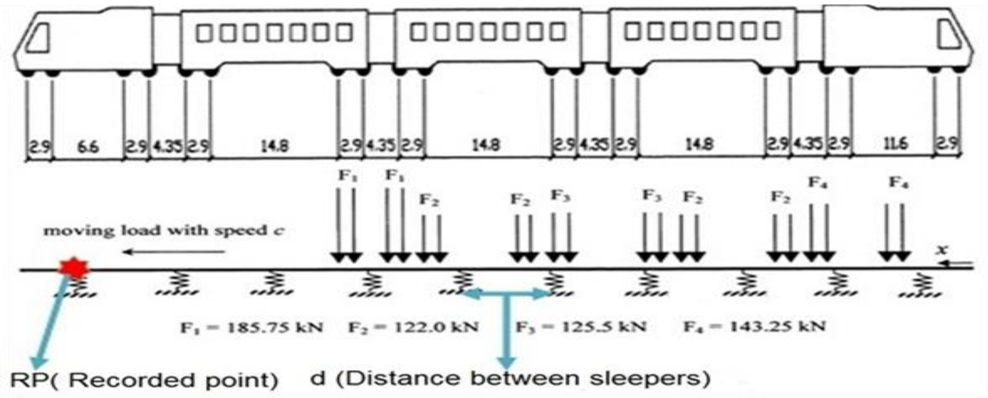

Figure2 , Top: sketch of the X-2000 train. Bottom: concentrated moving loads on an elastic beam with spring supports, and a recorded point. Picture taken from [6].

To estimate the spring stiffness ke, it was assumed that a typical value ke = Es is generally accepted for beam on elastic foundation [6] where Es is elastic module of soil. The best fit with observations was obtained using ke = 1.2Es that coincides with the value suggested by Gazetas et al. [13] for soil-pile interaction problems under transversal motion. As there was no information available on the frequency dependence of the spring stiffness, a constant value for ke was considered.
The parameters and material properties which were used in this problem are shown in table 1. Where, Lt is the length of train, Lr is the length of railway in model, Er Young's modulus of rail, Gr is the rail section shear modulus, ρr is the rail density, νr is the rail section Poisson's ratio, vt is the train velocity, d is the distance between sleepers, and dr is the distance between RP and head of the train.

Table 1, Parameters of the train and railway

Parameter	Parameter Type Unit	Parameter Type Unit
Type of train	X2000	-
L_t	109	m
L_r	200	m
E_r	2.1e11	pa
G_r	8.0769e10	pa
ρ_r	7850	Kg/m3
ν_r	0.3	-
Rail profile	UIC 60	-
v_t	200	km/h
d	50	cm
d_r	30	m

Time history responses

The results of the train movement on an elastic beam were divided in to time history function of displacement, velocity and acceleration which all were numerical functions. These functions were discrete functions and the accuracy of them depended on time steps. Figures

3(a), 3(b) and 3(c) show these functions between the time period 0 and 4 seconds. Furthermore, the velocity and acceleration function can be obtained by the equations (1) and (2) theoretically.

$$v(x,t)=\frac{\partial y(x,t)}{\partial t} \qquad (1)$$

$$a(x,t)=\frac{\partial^2 y(x,t)}{\partial t^2}=\frac{\partial v(x,t)}{\partial t} \qquad (2)$$

In figure 3(a), it is clear that displacements oscillated rapidly until 2.3 seconds and after that, the displacement dropped to the zero. At 0.438s, the maximum displacement happened. Moreover, there were twenty peaks which referred to the axles in the train. As shown in Fig 3(b), the velocity function had an amplitude in the range of -0.0495 m/s to 0.0967 m/s. Between 0.65 s to 1.41 s, there were not any sensible peaks. This means that the high amplitudes can be excited approximately, in the earlier moments and in the final of the train movement from RP. The numerical results of the train movement on an elastic beam was used as "Dynamic loading-Displacements" input data in Plaxis. Furthermore, in Fig 3(c), the maximum peak of acceleration occurred after 2 second meaning the highest impact of force happened at the end of movement.

Plaxis model

An elastic beam with three homogeneous linear elastic layers were considered, Fig 4. The elastic beam was a concrete sleeper and the upper layer was a ballast layer located at the bottom of the sleeper. The second layer was a sub ballast layer located between the ballast and the soil bed and finally the third one was the subsoil layer. For modelling in axisymmetry condition by Plaxis, all the length of layers were calculated in axisymmetry condition. Tables 2, 3, 4 and 5 provide the properties of beam and layers. In order to simulate the effects of the ambient excitation and to comprehend the dynamic behavior, time interval of 4 sec duration was used. In dynamic analysis, we modeled the soil layers as linear elastic materials. The soil layers did not experience the development of the plastic zones in the region of consideration. The geometry of the model was defined for a constant width of the soil layer with different domain depths. Horizontal fixities were used at the far-end of vertical boundaries, while the bottom boundary of the model, representing the existence of the bedrock, had been subjected to total fixity i.e. both horizontal and vertical fixities. Absorbent boundaries were introduced at the far vertical boundaries aiming to absorb the stresses on the boundaries caused by dynamic loading, that otherwise would be reflected back to the subsoil. Dynamic excitation was introduced by velocity amplitude at the soil layer of the model. In order to reduce vibrations, a concrete wave barrier was applied. The concrete barrier situated in the distance of 10 m from the track. The properties of the barrier can be seen in table 6. Since, the model chosen for the present study was uniform, the initial stresses in the model were generated considering at-rest condition. The domain was subdivided into two regions. The depth of the first region was equal to the quarter of total depth of the domain. Such a configuration with lateral domains was used in order to obtain the effect of vibrations on the specific points. Figure 5 depicts the schematic diagram of the dynamic model and boundary conditions to be analyzed. In order to diminish the wave reflection the bottom and right boundaries were modeled as absorbent boundaries.

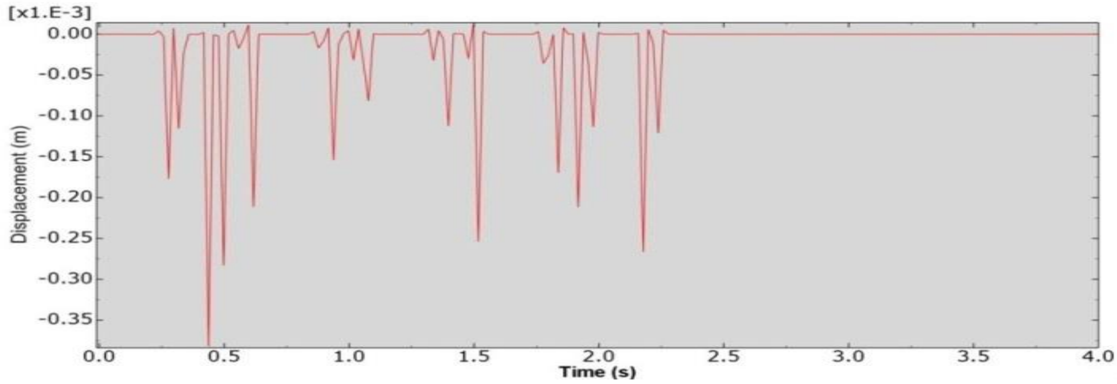

(a)

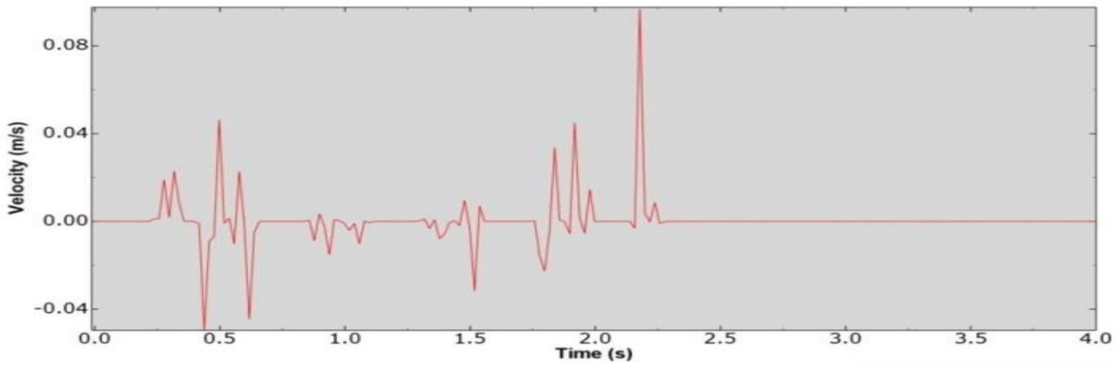

(b)

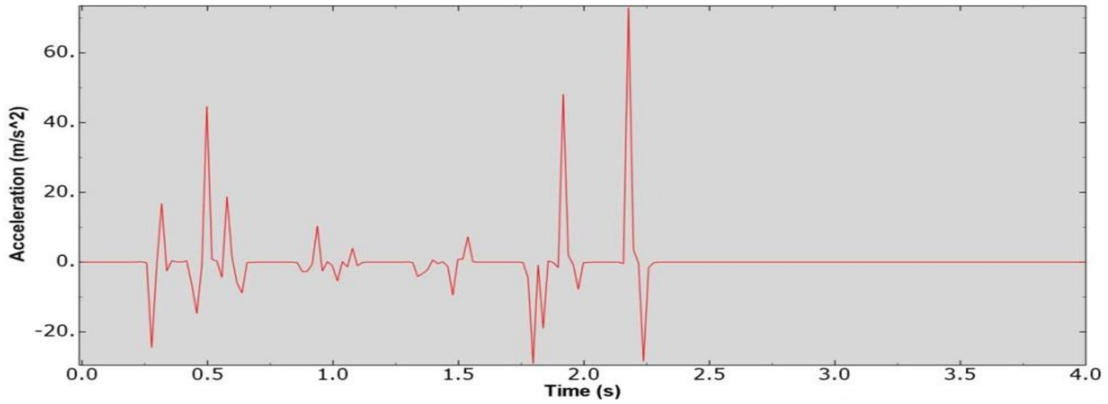

(c)

Figure3 , Time history reaction of RP (recorded point) during the movement of concentrated loads on an elastic beam with spring supports. (a) Time history-Vertical Displacement (b) Time history-Vertical Velocity (c) Time history- Vertical Acceleration.

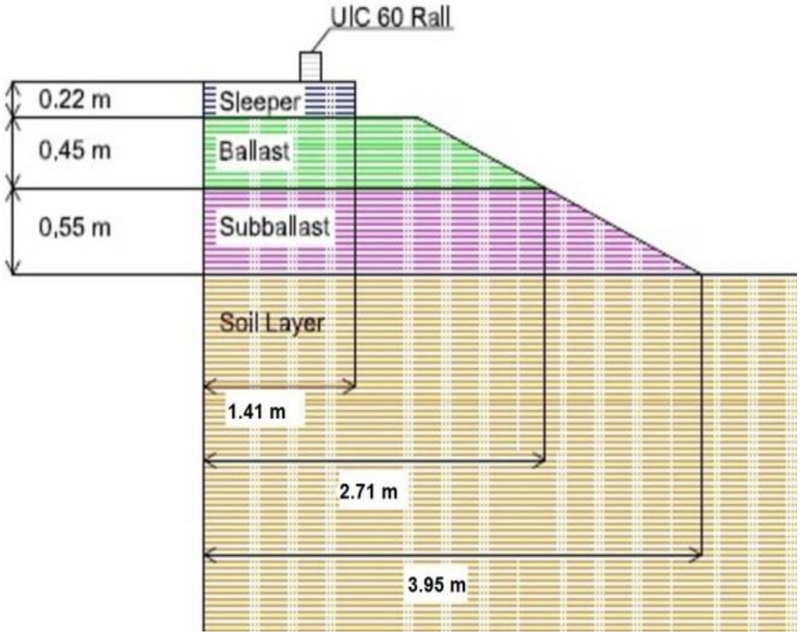

Figure4 , the railway embankments and subsoil cross section.

Table 2, Properties of the Sleeper

Parameter	Symbol	Magnitude/Unit
Half-length of sleeper	L_s	1.25 m
Normal stiffness	$(EA)_s$	7.5e7 KN/m
Flexural rigidity	$(EI)_s$	3e5 KNm^2/m
Poisson's Ratio	ν_s	0.2
weight	W_s	23.52 KN/m/m
Thickness of sleeper	d_s	219 m

Table 3, Properties of the Ballast

Parameter	Symbol	Magnitude/Unit
Height of the ballast	h_b	0.45 m
Unsaturated unit weight	γ_{unsat}	15.5 KN/m^3
Elastic modulus	E_b	9.7e4 KN/m^2
Poisson's Ratio	ν_b	0.12
Shear Modulus	G_b	4.33e4 KN/m^2
Oedometric Modulus	E_{oed}	10e4 KN/m^2
S-wave velocity	V_s	165 m/s
P-wave velocity	V_p	251.2 m/s

Table 4, Properties of the Sub ballast

Parameter	Symbol	Magnitude/Unit
Height of the sub ballast	H_{sb}	0.55 m
Unsaturated unit weight	γ_{unsat}	18.7 KN/m^3
Elastic modulus	E_{sb}	21.2e4 KN/m^2
Poisson's Ratio	N_{sb}	0. 2
Shear Modulus	G_{sb}	8.83e4 KN/m^2
Oedometric Modulus	E_{oed}	25.6e4 KN/m^2
S-wave velocity	V_s	215 m/s
P-wave velocity	V_p	351.2 m/s

Soil damping in Plaxis

As the calculations were performed in the time domain using direct time integration, the subsoil damping was modelled with the Rayleigh damping model. The damping ratio in the Rayleigh damping model was frequency dependent. The parameters in damping model were therefore chosen so that model had a damping ratio of about 3% in the frequency range of interest 5 to 15Hz. The damping relation with frequency used is shown in Equation (3) [11].

$$\alpha + \beta\omega_i^2 = 2\omega_i\varsigma_i \qquad \textbf{(3)}$$

This relation entails that if two damping ratios at given frequencies are known, two simultaneous equations can be formed, from which α and β can be calculated. In the domain of frequency 5 to 15 Hz and damping ratio 0.03, the damping coefficient were:

α= 1.41 and β= 4.78e-4

Table 5, Properties of the Soil layer

Parameter	Symbol	Magnitude/Unit
Height of the soil layer	H_{sb}	0.55 m
Unsaturated unit weight	γ_{unsat}	18.7 KN/m^3
Elastic modulus	E_{sb}	21.2e4 KN/m^2
Poisson's Ratio	N_{sb}	0. 2
Shear Modulus	G_{sb}	8.83e4 KN/m^2
Oedometric Modulus	E_{oed}	25.6e4 KN/m^2
S-wave velocity	V_s	215 m/s
P-wave velocity	V_p	351.2 m/s
Damping ratio	ζ	3%
Rayleigh α	α	1.41
Rayleigh β	β	4.78e-4

Table 6, Properties of the concrete barrier

Parameter	Symbol	Magnitude/Unit
Height of concrete	H_{sb}	7 m
Unsaturated unit weight	γ_{unsat}	25 KN/m^3
Elastic modulus	E_{sb}	2.5e7 KN/m^2
Poisson's Ratio	N_{sb}	0. 15
Shear Modulus	G_{sb}	1.087e7 KN/m^2
Oedometric Modulus	E_{oed}	2.640e7 KN/m^2
S-wave velocity	V_s	2064 m/s
P-wave velocity	V_p	3217 m/s
Damping ratio	ζ	4%
Rayleigh α	α	1.89
Rayleigh β	β	6.37e-4

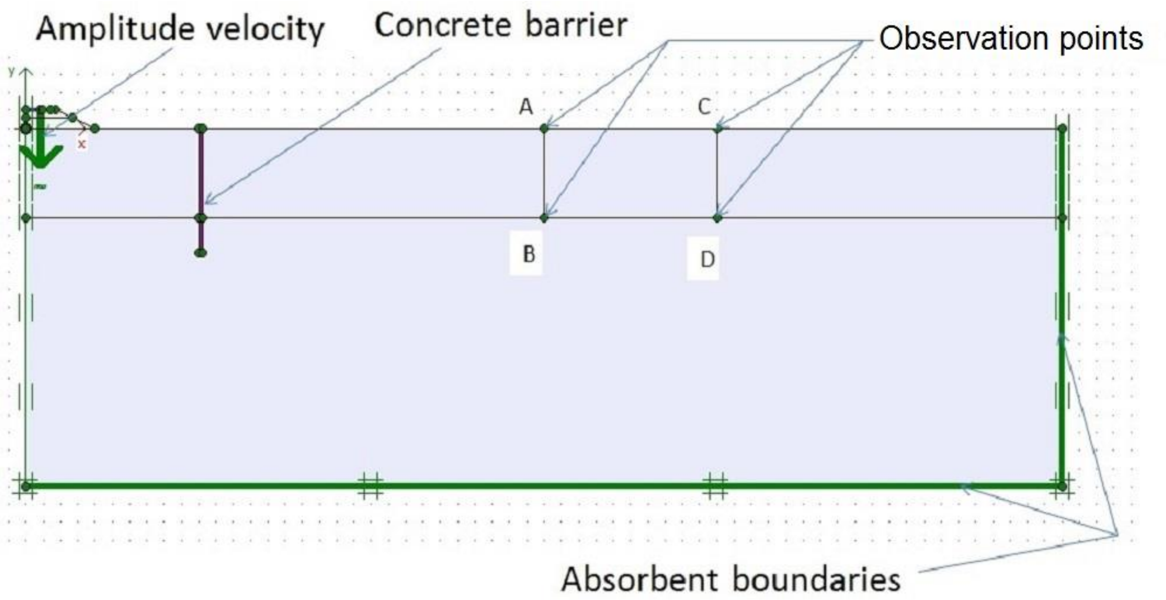

Figure 5, the sketch of boundary conditions (normal boundary+ absorbent boundaries) and the location of Amplitude velocity, Concrete barrier, and Observation points.

Finite element model

The finite element simulations of train-induced ground vibrations included a two-dimensional finite element model perpendicular to the track (axisymmetric model perpendicular model) with stationary loading that was used to study the ground response outside the embankment. This model could also generated a more realistic model of the wave propagation. The results from the finite element analyses without barrier were compared with the ones with barrier so that they could be analyzed and discussed. In this paper, only the results from the analyses of a train with a speed of 200 km/h were considered. The axisymmetric model, shown in Fig. 5, measured 20 x 60m2 and consisted of 722 elements and nodes. This was assumed as an initial estimate since only the response close to the track was considered. However, for analyses of the ground response at larger distances from the track, it was more important to have a wide model as the influence area of the moving load increases. The model consisted of a 6-node triangle for soil elements and a 3-node line for plate elements. Moreover, a three-point Gaussian method was implemented to integrate each element. In the embankment, smaller elements of varying geometries were used in order to model sleepers and the complex geometry of the embankment. The density of mesh in case of without barrier and with barrier are shown in Fig. 6 (a) and Fig. 6 (b).

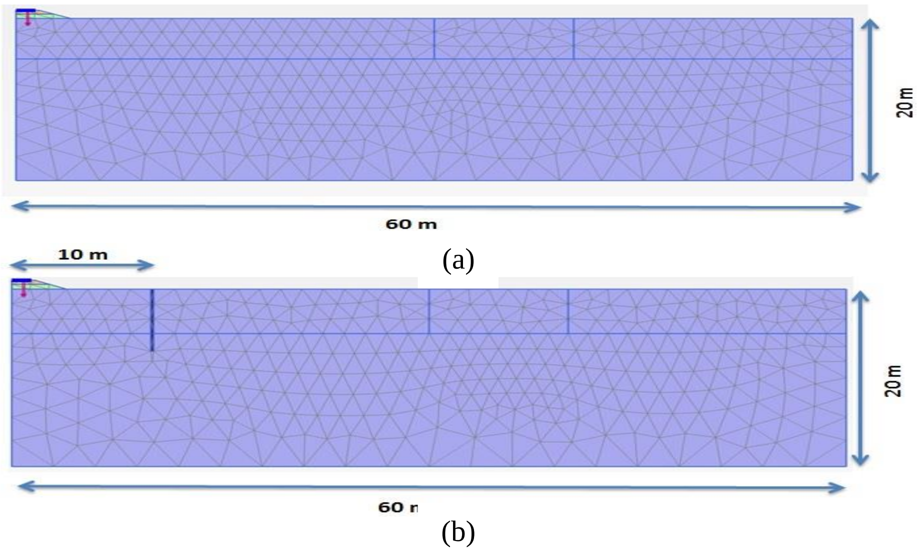

Figure6 , Mesh density and cross section. (a) Mesh density in case of without barrier with 722 elements and 1538 nodes (b) Mesh density in case of with barrier with 729 elements and 1546 nodes.

4. Results and Discussion

To model the effect of the wave barrier as a vibration reducer, observation points were employed. The location of each observation points from the railroad are shown in table 7. The results from the analyses of a train passing at a speed of 200 km/h are shown in Figs 7-10. It should be noted that blue and red lines in each figure are the results of modelling in case of without and with barrier respectively. Generally, in both case studies, the observation points located in the surface had particle velocities higher than the points located in the depth of 5 meter. For example in the case of without barrier, the maximum peak of total particle velocity in the observation point A was 2.54 mm/s. This value was bigger than the maximum peak in point B with magnitude of 1.62 mm/s. So, the vibrations in the surface were higher than the vibrations in the subsoil. Basically, the soil particles which were located in the surface had more degree of freedom than the particles in the interior layer.

According to the figures of particle velocity (Figs 7-10), the soil vibrations in all observation points with the wave barrier were reduced. Furthermore, to study the effectiveness of a concrete barrier in vibrations, the total particle velocity in both cases were compared. In the case of with barrier, the total velocity on point A (Fig 7(c)) mitigated around 12% in comparison with the total velocity in the case study without barrier. It seems that applying barrier had significant impact on mitigation of the surface wave than body wave. The excessive ground vibrations may have a significant impact on human comfort and on the built environment. Vibration annoys humans if the peak ground velocity (PGV) exceeds 2.5 mm/s, while a typical value for the onset of structural damage is 50 mm/s [6]. In the case study without barrier, the maximum total velocity at the observation point A exceeded this tolerable values (Figure 11). Thus, if there were any buildings on that distance, the inhabitants will annoy for the vibrations. However, in case study with barrier, the problem of vibrations was diminished in both upper part and inner part of the soil layer. Fig 11. Wave barrier seems to perform better in the upper part indicating that it reflexed and absorb surface waves rather than body waves.

Table 7, the location of observation points

Observation points	X-coordinate	Y-coordinate
A	30 m	0
B	30 m	-5 m
C	40 m	0
D	40 m	-5 m

5. Conclusion

The purpose of this study was to evaluate the dynamic behavior of a subsoil layer during wave propagation before and after constructing a concrete wave barrier. In the following study, we presented a detailed investigation on the mitigation of ground vibrations produced by a high-speed train with a concrete barrier to diminish vibrations.
By reviewing literatures, important factors to reduce ground vibration were extracted. These factors contain: particle ground velocity, soil shear velocity and also damping ratio. In the first part of modeling, to calculate the value of damping ratio of the subsoil layer and the concrete wave barrier, an analytical equation was used. The effectiveness of the concrete barrier was demonstrated through numerical modelling. The simulation has shown that the wave barrier was primarily responsible for the reduction. Simulation was made with a simple model. The wave barrier mitigated the velocity values. Besides, the use of concrete barriers reduced the ground vibrations significantly. In many practical cases it seems appropriate to perform a more detailed investigation of the structure/subsoil/barrier system under consideration of similar environmental dynamic conditions as it has been done in this modelling. Designing the optimum barrier with respect to its depth and width should be performed for each particular case. It is recommended that for buildings where sound and vibration isolation is critical, the modern methods for increasing the damping of the structure should be considered.

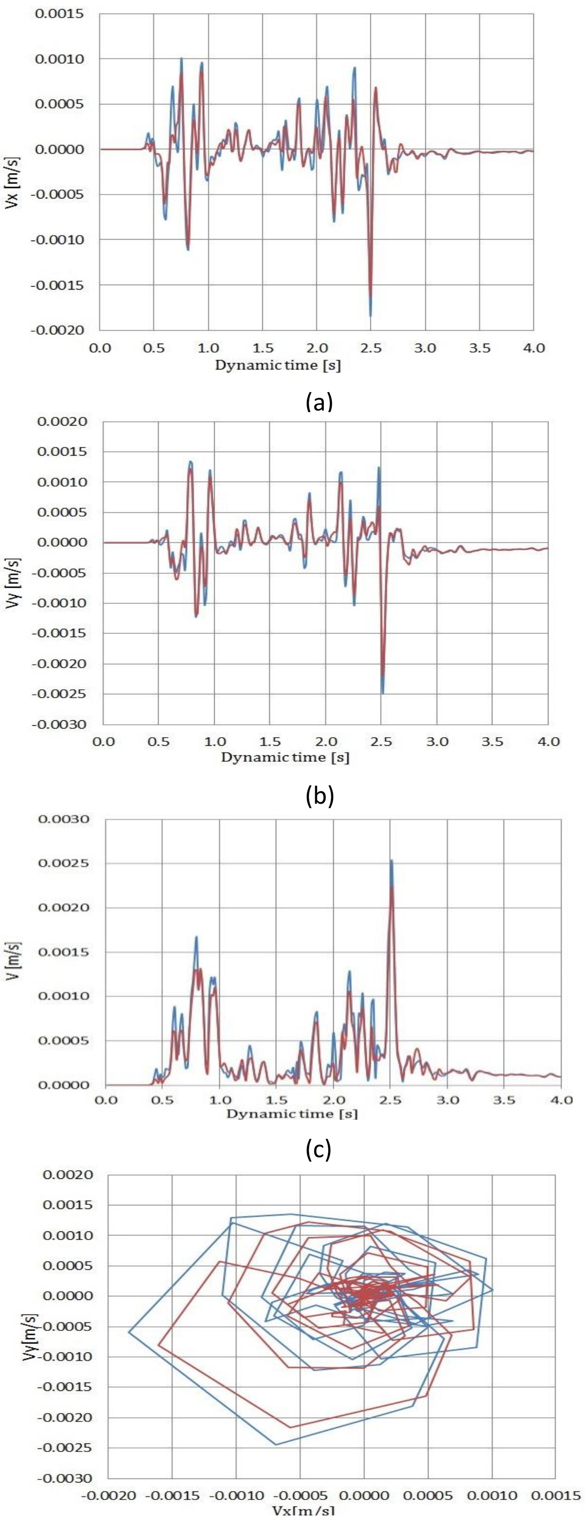

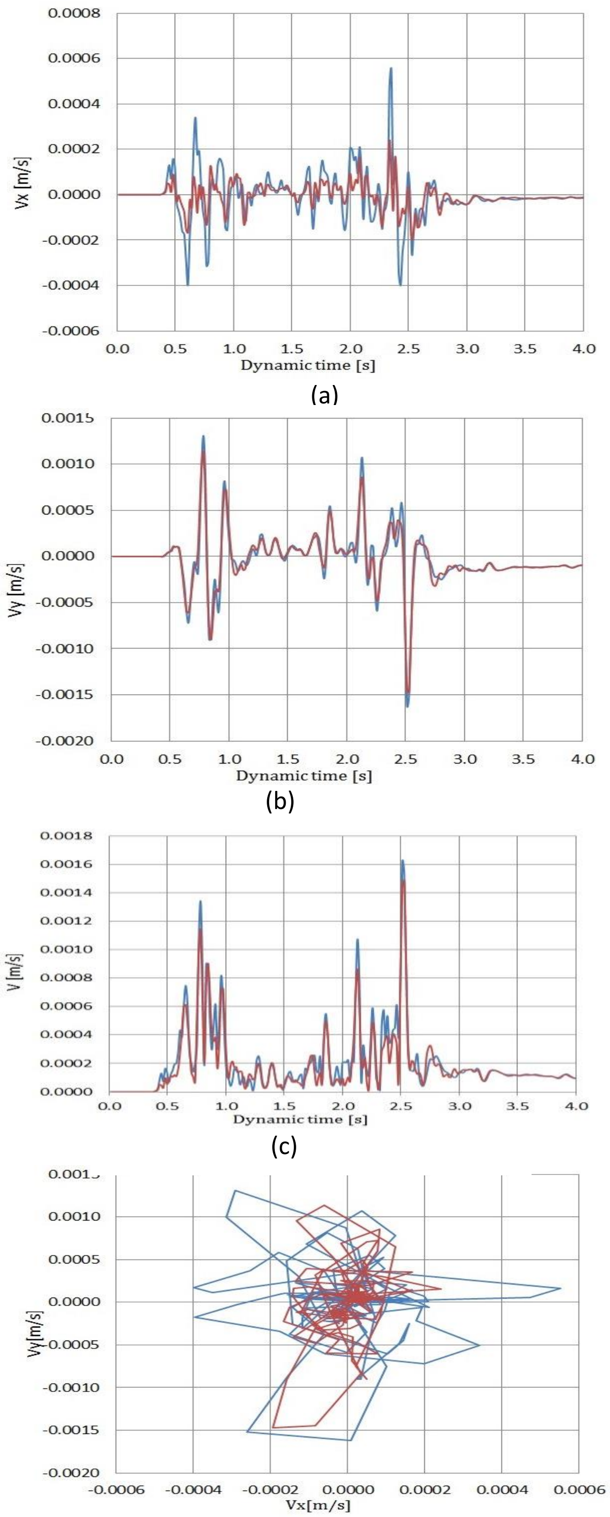

Figure7, Velocities on point A. (a) horizontal velocity responses. (b) Vertical velocity responses. (c) Total velocity responses. (d) Particle velocity responses.

Figure 8, Velocities on point B. (a) horizontal velocity responses. (b) Vertical velocity responses. (c) Total velocity responses. (d) Particle velocity responses.

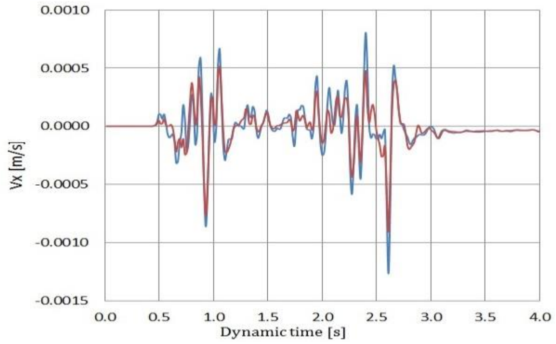

(a)

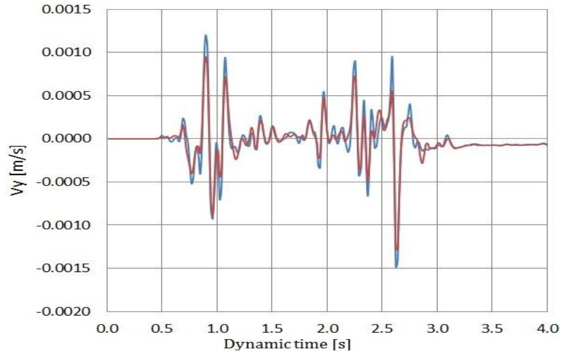

(b)

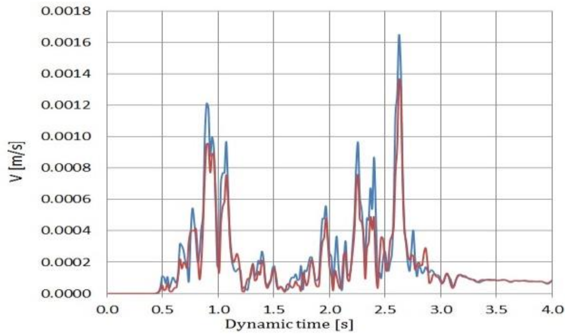

(c)

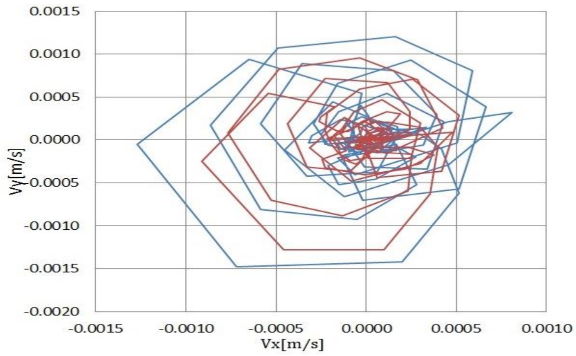

(d)

Figure 9, Velocities on point C. (a) horizontal velocity responses. (b) Vertical velocity responses. (c) Total velocity responses. (d) Particle velocity responses.

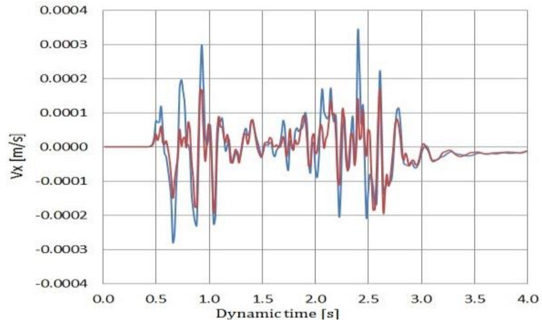

(c)

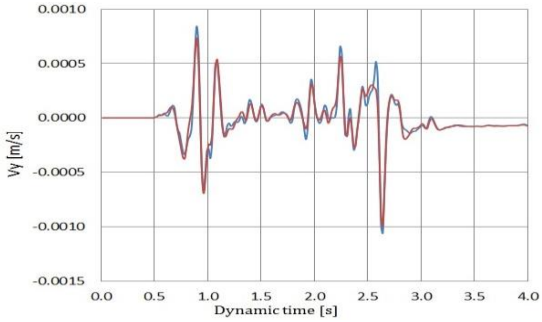

(b)

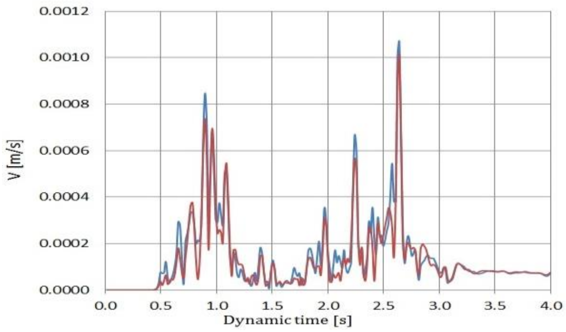

(a)

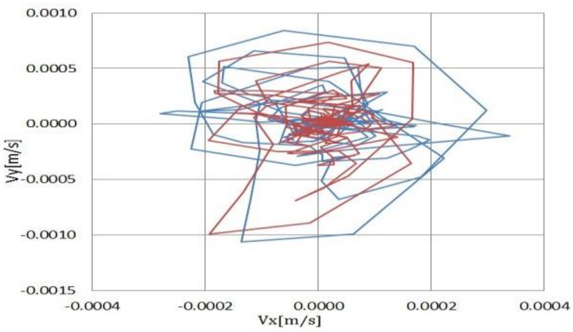

(d)

Figure 10, Velocities on point D. (a) horizontal velocity responses. (b) Vertical velocity responses. (c) Total velocity responses. (d) Particle velocity responses.

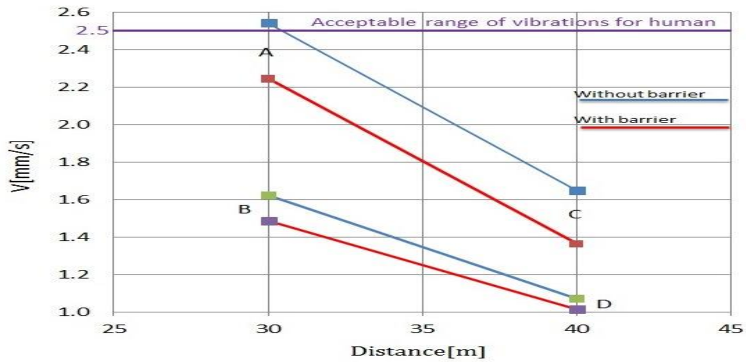

Figure 11, the impact of wave barrier on the maximum total velocity of observation points.

References

[1] Hall L. Simulations and analyses of train-induced ground vibrations in finite element models. Soil Dyn.Earthquake Eng. 2003;23(5):403-13.

[2] Khoubani A, Ahmadi MM. Discussion on the paper entitled: Numerical modeling of traffic-induced ground vibration. Comput.Geotech. 2013 1;47(0):102.

[3] Buonsanti M, Cirianni F, Leonardi G, Santini A, Scopelliti F. Mitigation of railway traffic induced vibrations: The influence of barriers in elastic half-space. Advances in Acoustics and Vibration 2009;2009.

[4] With C, Bahrekazemi M, Bodare A. Wave barrier of lime–cement columns against train-induced ground-borne vibrations. Soil Dyn.Earthquake Eng. 2009;29(6):1027-33.

[5] Alves Costa P, Calçada R, Silva Cardoso A. Ballast mats for the reduction of railway traffic vibrations. Numerical study. Soil Dyn.Earthquake Eng. 2012;42:137-50.

[6] Paolucci R, Maffeis A, Scandella L, Stupazzini M, Vanini M. Numerical prediction of low-frequency ground vibrations induced by high-speed trains at Ledsgaard, Sweden. Soil Dyn.Earthquake Eng. 2003 8;23(6):425-33.

[7] Krylov VV. Generation of ground vibrations by superfast trains. Appl.Acoust. 1995;44(2):149-64.

[8] Madshus C, Kaynia A. High-speed railway lines on soft ground: dynamic behaviour at critical train speed. J.Sound Vibrat. 2000;231(3):689-701.

[9] Forrest J, Hunt H. Ground vibration generated by trains in underground tunnels. J.Sound Vibrat. 2006;294(4):706-36.

[10] Karlström A, Boström A. Efficiency of trenches along railways for trains moving at sub-or supersonic speeds. Soil Dyn.Earthquake Eng. 2007;27(7):625-41.

[11] Galvín P, Domínguez J. Experimental and numerical analyses of vibrations induced by high-speed trains on the Córdoba–Málaga line. Soil Dyn.Earthquake Eng. 2009;29(4):641-57.

[12] Yaseri A, Bazyar MH, Hataf N. 3D coupled scaled boundary finite-element/finite-element analysis of ground vibrations induced by underground train movement. Comput.Geotech. 2014 7;60(0):1-8.

[13] Gazetas G, Dobry R. Horizontal response of piles in layered soils. J.Geotech.Eng. 1984;110(1):20-40.

[14] Brinkgreve R, Broere W. Dynamics. Plaxis: finite element code for soil and rock analyses: 2D-Version 8:[user's guide]; 2004, p. 7-8.